# Transport in exclusion processes with one-step memory: density dependence and optimal acceleration

OPEN ACCESS
IOP Publishing
Journal of Physics A: Mathematical and Theoretical
J. Phys. A: Math. Theor. **52** (2019) 385001 (19pp)
https://doi.org/10.1088/1751-8121/ab37e4

# Transport in exclusion processes with one-step memory: density dependence and optimal acceleration

**Eial Teomy and Ralf Metzler**

Institute for Physics & Astronomy, University of Potsdam, Karl-Liebknecht-Straße 24/25, D-14476 Potsdam-Golm, Germany

E-mail: eialteom@gmail.com

Received 8 July 2019
Accepted for publication 1 August 2019
Published 26 August 2019

**Abstract**

We study a lattice gas of persistent walkers, in which each site is occupied by at most one particle and the direction each particle attempts to move to depends on its last step. We analyse the mean squared displacement (MSD) of the particles as a function of the particle density and their persistence (the tendency to continue moving in the same direction). For positive persistence the MSD behaves as expected: it increases with the persistence and decreases with the density. However, for strong anti-persistence we find two different regimes, in which the dependence of the MSD on the density is non-monotonic. For very strong anti-persistence there is an optimal density at which the MSD reaches a maximum. In an intermediate regime, the MSD as a function of the density exhibits both a minimum and a maximum, a phenomenon which has not been observed before. We derive a mean-field theory which qualitatively explains this behaviour.

Keywords: exclusion process, persistence, lattice gas

(Some figures may appear in colour only in the online journal)

## 1. Introduction

The active and passive motion of biological cells and the motion of their internal components (molecular motors, enzymes, etc) is a complicated out-of-equilibrium process which occurs due to many factors, some of them still unknown [1]. This motion has been investigated at the

single-body level [2–4], many-body level [5–15], or continuum level [16]. At the many-body level the focus is mostly on the interactions between cells or bacteria, be they hydrodynamic [5], mutually aligning as in the Vicsek model [7, 8], energetic [8–11], or steric [12–15, 17].

The motions of individual cells or bacteria are modelled in various ways, which can be thought of as a random walk with a certain type of memory. One of the most common models, motivated by experimental observations [18], is a run-and-tumble motion [3, 10], in which the walker moves in a straight line for some time, and then abruptly changes its direction. This model is captured by a memory term which gives a higher probability of turning as more time passes from the last turn. A twitching motion [11] or motion with a self aligning director [13] is captured by a one-step memory term, i.e. the velocity at each step depends on the velocity in the previous step but not on longer memory terms. Other biological processes are also described as random walks with memory [19–21].

In random walks with memory, each step the walker makes depends not only on its location in the previous step but on its history. It might depend on its entire history, or a finite part of it. Notably, in one of the first and best known random walk models that included memory [22], a single walker moves on a one-dimensional lattice. At each step, the walker either moves in the same direction as it did in the previous step with probability $\frac{1}{2}+\delta$, or in the opposite direction with probability $\frac{1}{2}-\delta$. This rule mimics inertia, and does not introduce bias in any specific direction. The basic random walk model is retrieved for $\delta = 0$. Such walkers with one-step memory are also called persistent walkers. Since the introduction of this model, it was expanded in various forms to explain different phenomena in fields such as polymer chains [23], animal movement [24], scattering in disordered media [25], motion of bacteria [2], artificial micro-swimmers [26, 27], and motion in ordered media [28].

A different class of random walk models emulates the interactions in many-body systems. In these 'lattice-gas models' many walkers move on a discrete graph or lattice with some type of interaction between the different particles. In the simple symmetric exclusion principle (SSEP) model [29] the interaction is purely steric. Each site on a lattice is either vacant or occupied by at most one walker, and each walker has an internal clock, independent of the other walkers, which governs the timing of its attempted moves. If a walker attempts to move to an already occupied site, it remains in place. In the asymmetric simple exclusion principle (ASEP) model [29], the walkers are biased to move in a certain direction, and it has been used to describe transport phenomena in biology [14, 30, 31]. A special consideration is given to one-dimensional systems [32], which emulate transport along a narrow channel, such as transport of water [33] and drugs [34] through nanotubes, or of molecular motors in cellular protrusions [14] and along microtubules [30, 35]. The single file diffusion in one-dimensional systems is known to be anomalous, even without memory [36]. The basic SSEP and ASEP models have been expanded to include energetic interactions [37], a single biased particle surrounded by unbiased particles [38], birth and death of particles [39], higher site occupancy [40], spatial inhomogeneities [41] and kinetic constraints [42].

There are several studies that combine these two variations of the basic random walk, mutual exclusion effects and memory, and they investigate three characteristics of this type of models. First, this model may be considered as a coarse-grained version of active Brownian particles (ABP) [26], and it was shown that it indeed shows motility induced phase separation [43, 44], one of the hallmarks of ABP. Second, some studies derived an effective hydrodynamic description in either one-dimensional [45, 46] or higher-dimensional [47, 48] systems, including anomalous walkers [49]. The third group of studies investigates the mean squared displacement (MSD) of crowded walkers with memory, in particular the short time approximation of the MSD [50], the MSD of interacting subdiffusive random walkers in a

one-dimensional system [51], the MSD in the very high density limit in one dimension [52], and the effective diffusion coefficient of a cross-shaped persistent walker in a bath of memoryless cross-shaped walkers [53].

In this study we investigate the MSD of persistent random walkers in a crowded environment in both one-dimensional (1D) and two-dimensional (2D) systems. We perform simulations covering the entire parameter space and find that in general the MSD behaves as expected: it decreases with the density and increases with the persistence. However, for strong anti-persistence we find two different regimes, in which the dependence of the MSD on the density is non-monotonic. For very strong anti-persistence there is an optimal density at which the MSD reaches a maximum. In an intermediate regime, the MSD as a function of the density exhibits both a minimum and a maximum, a phenomenon which to our knowledge has not been observed before. We derive a mean-field theory which explains this phenomenon qualitatively. We also investigate the previously unexplored cases of totally persistent and totally anti-persistent particles, for which the density has a critical effect. On the one hand, a single totally persistent particle performs a ballistic motion, while remarkably in a system with finite density all movement halts after a transient time. On the other hand, a single totally anti-persistent walker is localised, while in a system with density larger than 1/2 its motion is unbounded.

The details of the model we investigate are described in section 2. Section 3 is devoted to the numerical analysis of the MSD under general conditions, while in sections 4 and 5 we consider the extreme cases of full persistence and full anti-persistence. Finally, section 6 summarises the paper. In the appendix we derive a computationally efficient method to calculate the MSD of a single particle with general memory, which we use in our mean-field theory.

## 2. Description of the model

We consider a lattice gas in either a 1D linear lattice or a 2D square lattice. Each site on the lattice can be either vacant or occupied by at most one particle. Each particle has an independent exponential clock with mean time $\tau$. When the clock rings, the particle attempts to move to one of its two (in 1D) or four (in 2D) nearest neighbours. If the target site is vacant, the particle moves. Otherwise, it remains in place. In both cases, its clock resets.

The target direction, however, is not chosen from a uniform distribution but it rather depends on the history of the particle. We consider here one-step memory models, also called persistent walkers. In the 1D model, pictured in figure 1(a), the probability that a particle attempts to move in the same direction as in its previous state is $\frac{1}{2}+\delta$ with $-\frac{1}{2}\leqslant\delta\leqslant\frac{1}{2}$, and the probability it reverses its direction is $\frac{1}{2}-\delta$. We call the parameter $\delta$ the persistence parameter, since it encodes the tendency of the particle to persist in its motion. Note that since the probability distribution for choosing the direction of motion is relative to the current direction of motion, there is no macroscopic bias in the system unless it is imposed from the boundaries. In the 2D model, pictured in figure 1(b), the probability that a particle attempts to move in the same direction as before is $\frac{1}{4}+\delta_f$, the probability that it attempts to move in the opposite direction is $\frac{1}{4}+\delta_b$, and the probability that it attempts to move in either of the other two directions is $\frac{1}{4}-\frac{\delta_f+\delta_b}{2}$, i.e. here $\delta_f$ is not necessarily equal to $-\delta_b$ as in one dimension[1].

[1] In higher dimensions the situation is similar to 2D: the probability to move forward is $\frac{1}{2d}+\delta_f$, the probability to move backwards is $\frac{1}{2d}+\delta_b$, and the probability to move to any of the other $2d-2$ directions is $\frac{1}{2d}-\frac{\delta_f+\delta_b}{2(d-1)}$. We expect the results for high dimensions to be qualitatively similar to two dimensions. Here we focus on the relevant 1D and 2D cases.

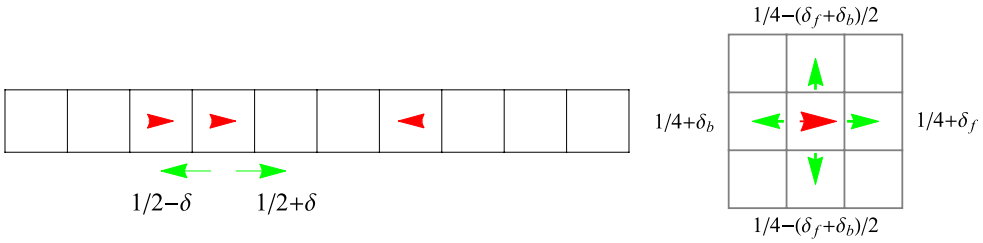


**Figure 1.** An illustration of the model. The last direction in which the particle moved is denoted by the red arrow. At each step the particle turns in one of the directions with probabilities shown near the green arrows, and moves in that direction if the target site is vacant. In 1D the system parameter is the persistence $\delta$, in 2D we classify the motion by the two parameters $\delta_f$ and $\delta_b$.

Note that although the net current is zero, this model is out of equilibrium because it does not obey detailed balance. Consider for example a particle moving to the vacant site to its right, and that in its previous step it also moved to the right. Such a move occurs with probability $\frac{1}{2}+\delta$ (in 1D) or $\frac{1}{4}+\delta_f$ (in 2D). The opposite transition, however, has a zero probability of occurring, since if the particle moves to the now vacant adjacent site to its left its last move was to the left, and it is thus in a different state than the one it started from.

In the simulations we perform, we use periodic boundary conditions and a system of either size $10^4$ (in 1D) or $100\times 100$ (in 2D). The initial state of the system is uncorrelated: each site is independently occupied with probability $\rho$, and the direction of each walker is independently and uniformly generated from the possible two (in 1D) or four (in 2D) directions. At each step of the simulation, one of the particles is chosen randomly and a move is attempted. Whether the move succeeds or not the clock advances by $\frac{\tau}{N}$, where $N$ is the number of particles in the system and we choose the time units to be $\tau=1$. This evolution is equivalent to each particle having an exponential clock with mean $\tau$. All results are averages of 100 independent runs.

## 3. Finite persistence

We first consider the non-pathological cases, i.e. that neither the probability to continue forward nor the probability to turn backward is exactly unity—we will consider these limiting cases below. Sample trajectories for three cases are shown in figure 2. Figure 3 shows sample trajectories in 2D, here we only depict a single particle's trajectory for clarity.

Without memory, it is known that in one dimensional systems the MSD scales as $\sqrt{t}$ [36], with the dependence on the density, for an equilibrium initial condition, given by

$$\left\langle x^2\right\rangle_{1\mathrm{D}}(t)=\frac{1-\rho}{\rho}\sqrt{\frac{2D_0t}{\pi}}, \tag{1}$$

where $D_0$ is the diffusion coefficient of a single walker. Note that for a single particle the MSD is linear in time $\left\langle x^2\right\rangle_{1\mathrm{D}}(t)=D_0t$ so that the limit $\rho\to 0$ drives the system across a transition. In two and higher dimensions, the MSD grows linearly with $t$, but the exact coefficient is unknown analytically [40, 54]. Furthermore, the MSD of a single particle with finite memory grows linearly with time in any dimension, since the velocity correlations decay exponentially. For one-step memory, the MSD of a single particle is [22, 23]

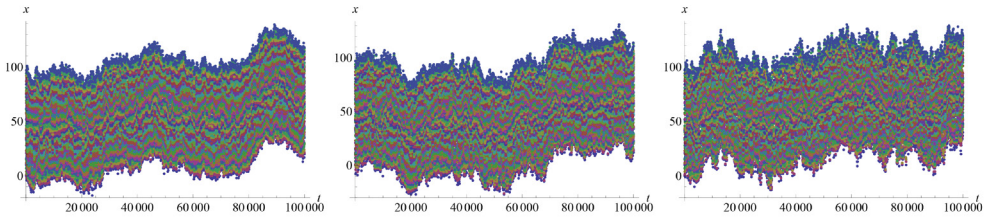


**Figure 2.** Sample trajectories of 1D systems with density $\rho = 0.4$. Left: anti-persistent case, $\delta = -0.2$; Middle: neutral case, $\delta = 0$; Right: persistent case, $\delta = 0.2$.

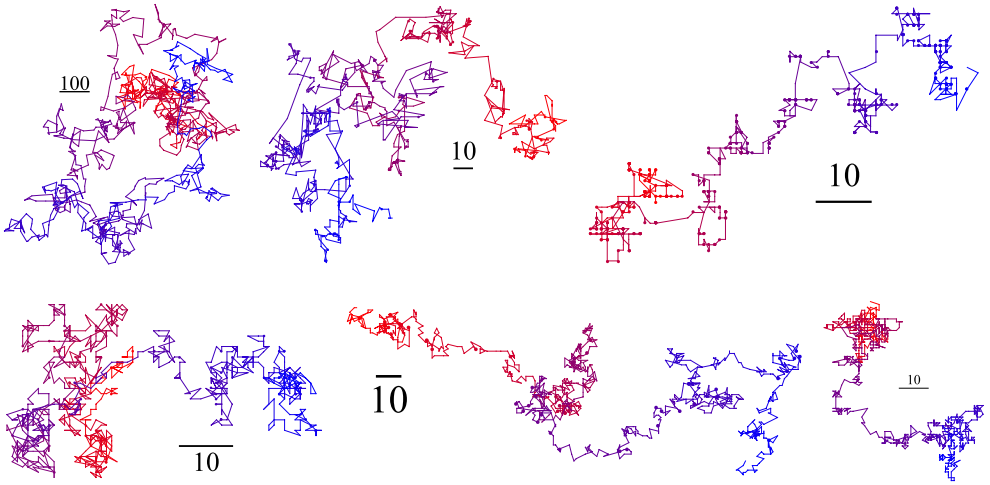


**Figure 3.** Sample trajectories of 2D systems for densities $\rho = 0.1$ (Left), $\rho = 0.6$ (Middle) and $\rho = 0.9$ (Right). In the top row the persistence parameters are $\delta_f = 0.45$ and $\delta_b = -0.50$ (highly persistent case), in the bottom row they are $\delta_f = -0.50$ and $\delta_b = 0.45$ (highly antipersistent case). The particle starts in the red region and ends in the blue region. The lengths of the black scale bars is given in lattice units. The different sizes of the scale bars give an impression of the overall span of the trajectories with respect to each other.

$$\langle x^2\rangle_{1D}(t) = D_0\frac{1+2\delta}{1-2\delta}t,$$
$$\langle \mathbf{r}^2\rangle_{2D}(t) = 2D_0\frac{1+\delta_f-\delta_b}{1-\delta_f+\delta_b}t, \tag{2}$$

where $D_0$ is the diffusion coefficient of a single walker without memory, and $\mathbf{r}^2 = x^2 + y^2$. Except for the pathological cases of full persistence and full anti-persistence, we find numerically that for all values of the persistence $\delta$ and the density $\rho$ the MSD in 1D systems grows as $\sqrt{t}$ and in 2D systems as $t$, see figure 4. The slope, however, becomes distinctly different from memory-less systems.

In 1D for each combination of the density $\rho$ and the persistence $\delta$ we use equation (1) and extract an effective diffusion coefficient $D_{\rm eff}$, as shown in figure 5, while in 2D we extract an effective diffusion coefficient from $\langle \mathbf{r}^2\rangle = 2D_{\rm eff}t$, see figure 6. Since for memory-less systems the MSD is a decreasing function of the density, and for single persistent walkers the MSD is

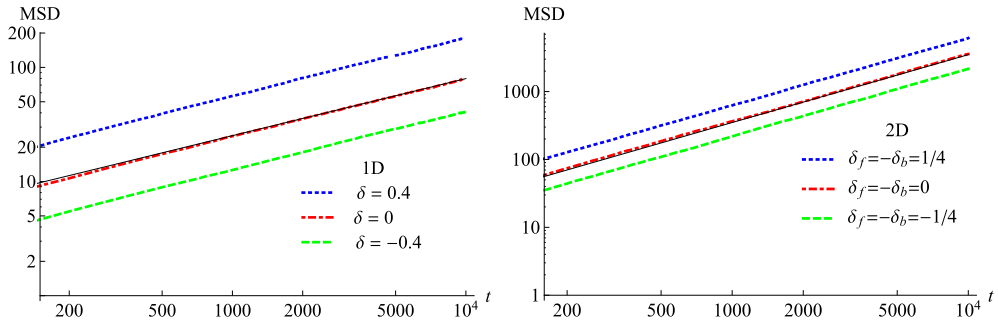


**Figure 4.** The MSD for a 1D and a 2D system with $\rho = 0.5$ and different persistence values. The continuous black line is the known result for $\delta = 0$ in 1D, equation (1), or a numerical fit in 2D. In all cases, the MSD grows with time as $\sqrt{t}$ for 1D and as $t$ for 2D.

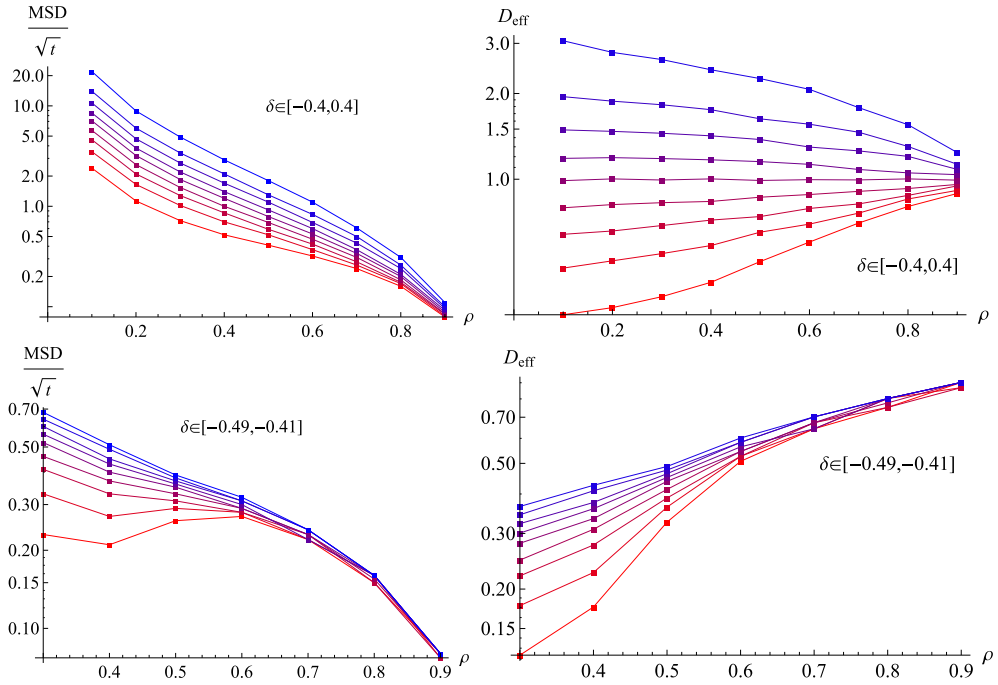


**Figure 5.** Log-plots of the slope of the MSD curve in 1D and the extracted diffusion coefficient as a function of the density $\rho$ for different values of the persistence $\delta$ from $\delta = 0.4$ (top line in blue) to $\delta = -0.4$ (bottom line in red) in jumps of 0.1 in the top panels, and from $\delta = -0.49$ (top line in blue) to $\delta = -0.41$ (bottom line in red) in jumps of 0.01 in the bottom panels.

an increasing function of the persistence, we expect that this dependence remains when both density and persistence are involved. Indeed, in 1D, we find that the effective diffusion coefficient is always a monotonically decreasing function of the persistence $\delta$, while in 2D it is a monotonically decreasing function of $\delta_f$ and a monotonically increasing function of $\delta_b$, as intuitively expected. Furthermore, in 1D it is an increasing function of the density for $\delta < 0$ and a decreasing function of the density for $\delta > 0$.

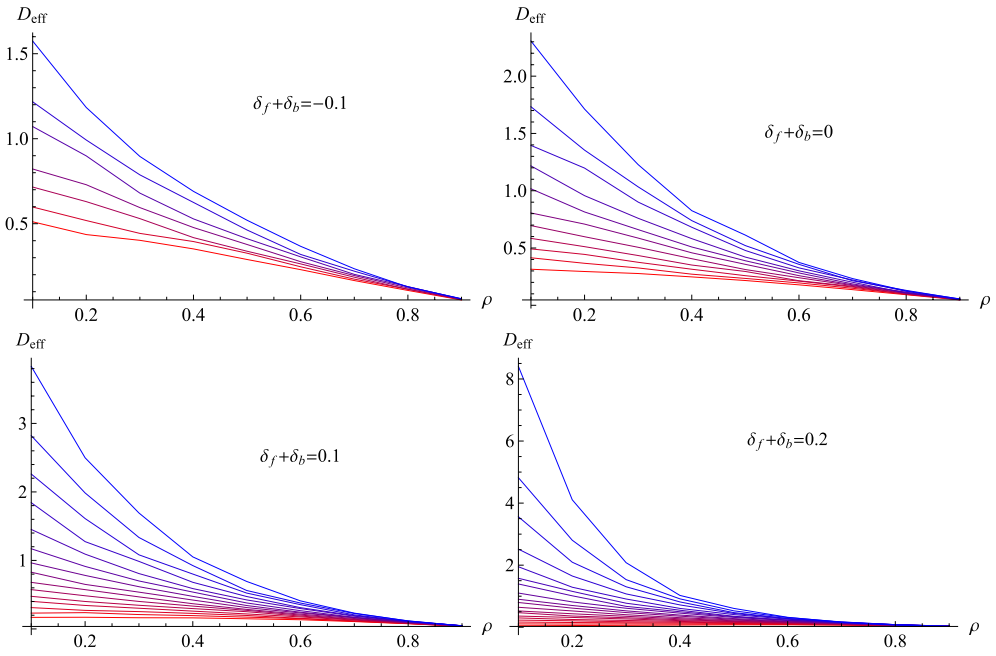


**Figure 6.** Diffusion coefficient for the 2D one-step memory model as a function of the density $\rho$ for various values of $\delta_f$ and $\delta_b$ and fixed $\delta_f+\delta_b$. The different lines correspond to different values of $\delta_f$ and $\delta_b$. In each plot the top line (in blue) is for $\delta_b=-0.25$ and the bottom line (in red) is for $\delta_f=-0.25$. For example, the lines for $\delta_f+\delta_b=-0.1$ are (from top to bottom) $(\delta_b=-0.25,\delta_f=0.35)$, $(\delta_b=-0.2,\delta_f=0.3),...,(\delta_b=0.35,\delta_f=-0.25)$. The limit at $\rho\to 0$ agrees with the single particle values.

We now look at the dependence of $\langle x^2\rangle/\sqrt{t}$ in 1D and of $\langle \mathbf{r}^2\rangle/t$ in 2D on the density. In most cases, it is a decreasing function of the density. However, at strong anti-persistence ($\delta\leqslant -0.48$ in 1D and $\delta_b\geqslant 0.55$ and $\delta_f\leqslant -0.19$ in 2D), remarkably we find two other types of density dependence. In that regime, the MSD may either have a single maximum as a function of the density (for example, as in $\delta_f=-0.25$ and $\delta_b=0.65$), or it may have both a maximum and a minimum (as in $\delta_f=-0.22$ and $\delta_b=0.62$), see figure 7. We note that in 1D, the single maximum regime occurs only for totally anti-persistent particles ($\delta=-1/2$), as will be explained below.

A similar peak in the MSD as a function of density was also found in a lattice model of a single biased tracer surrounded by regular random walkers [15, 55], but to our knowledge no other model exhibits the more complicated behaviour of both a maximum and a minimum. This behaviour is a competition between three mechanisms. The first, simplest mechanism occurs at high densities and is simply the blocking of the movement of the particles by their neighbours which reduces the MSD. The second mechanism is different in 1D systems and in higher dimensional systems, but in both cases it occurs at low densities. In 1D the MSD of a single particle scales linearly with $t$ while the MSD in a system with finite density scales as $\sqrt{t}$ due to the known effects of single file diffusion [36, 56]. Therefore, the MSD divided by $\sqrt{t}$ diverges at $\rho=0$, and thus for very small densities it is a decreasing function of $\rho$. In higher dimensions, the explanation is different since both the single particle MSD and the MSD in a finite density system are linear in time. In this case, when the anti-persistence is not too high

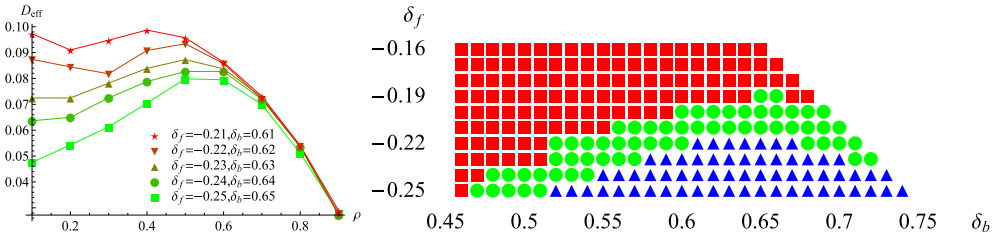


**Figure 7.** (a) Diffusion coefficient for the 2D one-step memory model as a function of the density $\rho$ for various values of $\delta_f$ and $\delta_b$. The connecting lines are a guide to the eye. When $\delta_f$ is small and $\delta_b$ is large, $D$ is not monotonic with $\rho$. (b) Phase diagram in the $\delta_b - \delta_f$ plane showing for each value whether the MSD is monotonically decreasing with $\rho$ (red squares), has a single maximum (blue triangles), or has both a maximum and a minimum (green circles).

and the density is low, the collisions between the particles are rare, and thus the only effect of the density is to occasionally block the movement, and thus reduce the MSD.

The intriguing third mechanism becomes relevant at high degrees of anti-persistence. In this mechanism, a particle is prevented from moving backwards by other particles that reach the site it occupied before, and thus in effect force it to move forward. In order to explain this behaviour qualitatively, we consider a single tracer starting at the origin. The other particles are acting as an effective bath, such that each move succeeds with probability $1-\rho$ and fails with probability $\rho$. We consider this mean-field description in 1D and 2D.

In 1D the time evolution of the probability to find the particle at time $t$ in site $n$ such that in the last step it moved in direction $\sigma = \pm 1$, $Q_\sigma(n,t)$, is

$$\tau \frac{\partial Q_\sigma(n,t)}{\partial t} = -Q_\sigma(n,t) + \left(\frac{1}{2}+\delta\right)\left[\rho Q_\sigma(n,t) + (1-\rho)\, Q_\sigma(n-\sigma,t)\right] + \left(\frac{1}{2}-\delta\right)\left[\rho Q_{-\sigma}(n,t) + (1-\rho)\, Q_{-\sigma}(n-\sigma,t)\right]. \tag{3}$$

Using the discrete Fourier transform of $Q_\sigma(n,t)$

$$\tilde{Q}_\sigma(k,t) = \sum_{n=-\infty}^{\infty} \mathrm{e}^{\mathrm{i}nk} Q_\sigma(n,t), \tag{4}$$

yields

$$\tau \frac{\partial \tilde{Q}_\sigma(k,t)}{\partial t} = -\tilde{Q}_\sigma(k,t) + \left(\frac{1}{2}+\delta\right)\left[\rho \tilde{Q}_\sigma(k,t) + (1-\rho)\, \mathrm{e}^{\mathrm{i}\sigma k}\tilde{Q}_\sigma(k,t)\right] + \left(\frac{1}{2}-\delta\right)\left[\rho \tilde{Q}_{-\sigma}(k,t) + (1-\rho)\, \mathrm{e}^{\mathrm{i}\sigma k} Q_{-\sigma}(k,t)\right]. \tag{5}$$

In matrix form this may be written as

$$\tau \frac{\partial}{\partial t}\begin{pmatrix}\tilde{Q}_+\\ \tilde{Q}_-\end{pmatrix} = \mathcal{M}_1(k)\begin{pmatrix}\tilde{Q}_+\\ \tilde{Q}_-\end{pmatrix}, \tag{6}$$

with

$$\mathcal{M}_1(k) = \begin{pmatrix} -1 + \left(\frac{1}{2}+\delta\right)\left[\rho + (1-\rho)\,\mathrm{e}^{\mathrm{i}k}\right] & \left(\frac{1}{2}-\delta\right)\left[\rho + (1-\rho)\,\mathrm{e}^{\mathrm{i}k}\right] \\ \left(\frac{1}{2}-\delta\right)\left[\rho + (1-\rho)\,\mathrm{e}^{-\mathrm{i}k}\right] & -1 + \left(\frac{1}{2}+\delta\right)\left[\rho + (1-\rho)\,\mathrm{e}^{-\mathrm{i}k}\right] \end{pmatrix}. \tag{7}$$

Therefore

$$\begin{pmatrix} \tilde{Q}_+(k,t) \\ \tilde{Q}_-(k,t) \end{pmatrix} = \mathrm{e}^{\mathcal{M}_1(k)t/\tau} \begin{pmatrix} \tilde{Q}_+(k,0) \\ \tilde{Q}_-(k,0) \end{pmatrix}. \tag{8}$$

In order to find $\tilde{Q}_\sigma(k,0)$ we note that by its definition

$$\tilde{Q}_\sigma(k,0) = \sum_{n=-\infty}^{\infty} \mathrm{e}^{\mathrm{i}nk} Q_\sigma(n,0) = \sum_{n=-\infty}^{\infty} \mathrm{e}^{\mathrm{i}nk} \frac{1}{2}\delta_{n,0} = \frac{1}{2}. \tag{9}$$

The MSD is given by

$$\begin{aligned} \left\langle n^2 \right\rangle &= -\frac{\partial^2}{\partial k^2}\left[\tilde{Q}_+(k,t) + \tilde{Q}_-(k,t)\right]\Big|_{k=0} \\ &= \frac{4\delta\,(1-\rho)^2}{(1-2\delta)^2}\left(\mathrm{e}^{-(1-2\delta)t/\tau} - 1\right) + (1-\rho)\left(1 + \frac{4\delta\,(1-\rho)}{1-2\delta}\right)\frac{t}{\tau}. \end{aligned} \tag{10}$$

The long time MSD is monotonically decreasing with the density for all $\delta \geqslant -\frac{1}{6}$, while for $\delta < -\frac{1}{6}$ it has a single maximum at $\rho = \frac{1+6\delta}{8\delta}$.

We now consider a persistent walker in 2D, such that each move succeeds with probability $1-\rho$ and fails with probability $\rho$. The evolution equation for the probability to find the walker at site $\mathbf{n}$ at time $t$, such that in the last step it moved in direction $\mathbf{e}$, $Q_{\mathbf{e}}(\mathbf{n},t)$ is

$$\begin{aligned} \tau\frac{\partial Q_{\mathbf{e}}(\mathbf{n},t)}{\partial t} =& -Q_{\mathbf{e}}(\mathbf{n},t) + \left(\frac{1}{4}+\delta_f\right)\left[\rho Q_{\mathbf{e}}(\mathbf{n},t) + (1-\rho)\,Q_{\mathbf{e}}(\mathbf{n}-\mathbf{e},t)\right] \\ &+ \left(\frac{1}{4}+\delta_b\right)\left[\rho Q_{-\mathbf{e}}(\mathbf{n},t) + (1-\rho)\,Q_{-\mathbf{e}}(\mathbf{n}-\mathbf{e},t)\right] \\ &+ \left(\frac{1-2(\delta_f+\delta_b)}{4}\right)\sum_{s=\pm1}\left[\rho Q_{s\mathbf{e}^\perp}(\mathbf{n},t) + (1-\rho)\,Q_{s\mathbf{e}^\perp}(\mathbf{n}-\mathbf{e},t)\right], \end{aligned} \tag{11}$$

where $\mathbf{e}^\perp = \mathbf{e}_y$ if $\mathbf{e} = \pm\mathbf{e}_x$, and $\mathbf{e}^\perp = \mathbf{e}_x$ if $\mathbf{e} = \pm\mathbf{e}_y$. Using the Fourier transform of $Q_{\mathbf{e}}(\mathbf{n},t)$

$$\tilde{Q}_{\mathbf{e}}(\mathbf{k},t) = \sum_{n_x,n_y=-\infty}^{\infty} \mathrm{e}^{\mathrm{i}\mathbf{n}\cdot\mathbf{k}} Q_{\mathbf{e}}(\mathbf{n},t), \tag{12}$$

yields

$$\begin{aligned} \tau\frac{\partial \tilde{Q}_{\mathbf{e}}(\mathbf{k},t)}{\partial t} =& -\tilde{Q}_{\mathbf{e}}(\mathbf{k},t) + \left(\frac{1}{4}+\delta_f\right)\left[\rho\tilde{Q}_{\mathbf{e}}(\mathbf{k},t) + (1-\rho)\,\mathrm{e}^{\mathrm{i}\mathbf{e}\cdot\mathbf{k}}\tilde{Q}_{\mathbf{e}}(\mathbf{k},t)\right] \\ &+ \left(\frac{1}{4}+\delta_b\right)\left[\rho\tilde{Q}_{-\mathbf{e}}(\mathbf{k},t) + (1-\rho)\,\mathrm{e}^{\mathrm{i}\mathbf{e}\cdot\mathbf{k}}Q_{-\mathbf{e}}(\mathbf{k},t)\right] \\ &+ \left(\frac{1-2(\delta_f+\delta_b)}{4}\right)\sum_{s=\pm1}\left[\rho\tilde{Q}_{s\mathbf{e}^\perp}(\mathbf{k},t) + (1-\rho)\,\mathrm{e}^{\mathrm{i}\mathbf{e}\cdot\mathbf{k}}Q_{s\mathbf{e}^\perp}(\mathbf{k},t)\right]. \end{aligned} \tag{13}$$

In matrix form this may be written as

$$\tau\frac{\partial}{\partial t}\begin{pmatrix}\tilde{Q}_x\\ \tilde{Q}_{-x}\\ \tilde{Q}_y\\ \tilde{Q}_{-y}\end{pmatrix}=\mathcal{M}_2(k)\begin{pmatrix}\tilde{Q}_x\\ \tilde{Q}_{-x}\\ \tilde{Q}_y\\ \tilde{Q}_{-y}\end{pmatrix}. \tag{14}$$

Therefore

$$\begin{pmatrix}\tilde{Q}_x(\mathbf{k},t)\\ \tilde{Q}_{-x}(\mathbf{k},t)\\ \tilde{Q}_y(\mathbf{k},t)\\ \tilde{Q}_{-y}(\mathbf{k},t)\end{pmatrix}=\mathrm{e}^{\mathcal{M}_2(k)t/\tau}\begin{pmatrix}\tilde{Q}_x(\mathbf{k},0)\\ \tilde{Q}_{-x}(\mathbf{k},0)\\ \tilde{Q}_y(\mathbf{k},0)\\ \tilde{Q}_{-y}(\mathbf{k},0)\end{pmatrix}. \tag{15}$$

In order to find $\tilde{Q}_{\mathbf{e}}(\mathbf{k},0)$ we note that by its definition

$$\tilde{Q}_{\mathbf{e}}(\mathbf{k},0)=\sum_{n_x,n_y=-\infty}^{\infty}\mathrm{e}^{\mathrm{i}\mathbf{n}\cdot\mathbf{k}}Q_{\mathbf{e}}(\mathbf{n},0)=\sum_{n_x,n_y=-\infty}^{\infty}\mathrm{e}^{\mathrm{i}\mathbf{n}\cdot\mathbf{k}}\frac{1}{4}\delta_{\mathbf{n},0}=\frac{1}{4}. \tag{16}$$

The long time limit of the MSD is given by

$$\begin{aligned}\left\langle\mathbf{n}^2\right\rangle&=-\nabla_k^2\sum_{\mathbf{e}}\tilde{Q}_{\mathbf{e}}(\mathbf{k},t)\Big|_{k=0}\\&=\frac{1-\rho}{1+\delta_b-\delta_f}\left[1+(1-2\rho)(\delta_f-\delta_b)\right]\frac{t}{\tau}.\end{aligned} \tag{17}$$

The calculation was done using a computationally efficient method described in the appendix. The MSD is a monotonically decreasing function of the density for $\delta_f-\delta_b>-\frac{1}{3}$, while for $\delta_f-\delta_b<-\frac{1}{3}$ it has a single peak at $\rho=\frac{3}{4}+[4(\delta_f-\delta_b)]^{-1}$.

Not surprisingly, based on a mean field description equations (10) and (17) can only give a qualitative picture of the mechanisms behind the non-monotonicity of the diffusivity. In particular, in 1D the scaling of the MSD with time is different. Even in 2D, the diffusion coefficient obtained from equation (17) does not agree too well with the simulation results. Furthermore, while the mean field result accounts for the single maximum scenario and therefore provides some added value in understanding our observations above, it cannot capture the strongly non-monotonic regime. Less severely, it does not provide the correct value of the persistence at the critical point. Moreover, we see from figure 5(b) that the behaviour in 2D depends on $\delta_f$ and $\delta_b$ in a more complicated manner than simply as $\delta_f-\delta_b$.

## 4. Full persistence

We now investigate the limiting case of full persistence in 1D. In this case, the model may be thought of as a two-species totally antisymmetric exclusion principle (TASEP), with equal populations of right-moving and left-moving particles. In this model, all motion stops after a short, density-dependent relaxation time, since a particle stops moving as soon as it encounters a block containing at least one other particle of the opposite species.

In order to investigate the motion of, say, a right-moving particle, it is sufficient to consider its nearest left-moving particle to the right of it and all the intervening right-moving particles, since all the other particles cannot affect its motion. Let us consider a right-moving particle

starting from the origin. At time $t = 0$, its nearest left-moving particle (to the right of it) is located at site $n$ with probability

$$q(n) = \left(1 - \frac{\rho}{2}\right)^{n-1} \frac{\rho}{2}. \tag{18}$$

Let us assume at first that there are no other right-moving particles between them. Note that until they encounter each other, the movement of the two particles is completely uncorrelated. Therefore, the probability that the right-moving particle is at site $m$ at time $t$ given that its nearest left-moving particle started at $n$, $p(m, n, t)$, is given by

$$\begin{aligned} p(m,n,t) = p_0(m,t) &\sum_{m'=0}^{n-m-1} p_0(m',t) \\ &+ \int_0^t \mathrm{d}t' \int_{t'}^t \mathrm{d}t'' p_0(m,t') \left(1 - \mathrm{e}^{-(t''-t')/\tau}\right) p_0(n-m-1,t'') \\ &+ \int_0^t \mathrm{d}t' \int_{t'}^t \mathrm{d}t'' p_0(m,t'') \left(1 - \mathrm{e}^{-(t''-t')/\tau}\right) p_0(n-m-1,t'), \end{aligned} \tag{19}$$

where $p_0(m, t)$ is the probability that a single independent walker moved $m$ steps at time $t$. The first term corresponds to the probability that at time $t$ the right-moving walker reaches site $m$ and the left-moving walker reached at most site $n - m - 1$, so they did not interact yet. The second term is the probability that the right-moving walker reached site $m$ at some time $t'$, and did not move until time $t''$ at which point the left-moving particle reached site $n - m - 1$. The last term is analogous to the second term, with the left-moving particle arriving first. The probability for an independent walker, $p_0(m, t)$, is governed by the evolution equation

$$\tau \frac{\partial p_0(m,t)}{\partial t} = -p_0(m,t) + p_0(m-1,t), \tag{20}$$

with the initial condition $p_0(m, 0) = \delta_{m,0}$, and therefore

$$p_0(m,t) = \mathrm{e}^{-t/\tau} \left(\frac{t}{\tau}\right)^m \frac{1}{m!}. \tag{21}$$

Using (21) in (19) yields

$$p(m,n,t) = \frac{(n+1)\left[n! - \Gamma\left(n+1, \frac{2t}{\tau}\right)\right]}{2^{n+1}\,(n-m)!\,(m+1)!} + \mathrm{e}^{-t/\tau} \left(\frac{t}{\tau}\right)^m \frac{\Gamma\left(n-m, \frac{t}{\tau}\right)}{m!\,(n-m-1)!}, \tag{22}$$

where $\Gamma(n, z)$ is the incomplete gamma function [57]. Summing over all possible initial locations for the left moving particle yields

$$\begin{aligned} p(m,t) = \sum_{n=m+1}^{\infty} p(m,n,t) q(n) &= \rho \left(1 - \frac{\rho}{2}\right)^{m-1} \left(\frac{1}{\left(1 + \frac{\rho}{2}\right)^{m+2}} - \frac{1}{2^{m+2}}\right) \\ &+ \mathrm{e}^{-(1+\rho/2)t/\tau} \left(\frac{t}{\tau}\right)^m \left(1 - \frac{\rho}{2}\right)^m \frac{1}{(m+1)!} \left(m + 1 - \frac{\rho}{2+\rho} \frac{t}{\tau}\right) \\ &+ \frac{\rho}{m!\,(4-\rho^2)} \left(\frac{t}{\tau}\right)^{m+1} \left(1 - \frac{\rho}{2}\right)^m \left[(2+\rho) E_{-m}\left(\frac{2t}{\tau}\right) - 4E_{-m}\left(\frac{t(1+\rho/2)}{\tau}\right)\right], \end{aligned} \tag{23}$$

where $E_\nu(z)$ is the exponential integral $E$ [58]

$$E_\nu(z) = \int_1^\infty \frac{\mathrm{e}^{-zt}}{t^\nu}\mathrm{d}t. \tag{24}$$

The MSD of such a right-moving particle without any intervening other right-moving particles is thus

$$\begin{aligned}\langle x^2\rangle_0 &= \sum_{n=1}^{\infty} m^2 p(m,t) = \frac{2\,(2-\rho)\left(4+6\rho+4\rho^2-\rho^3\right)}{\rho^2\,(2+\rho)^3} \\ &+ \left[\frac{2\rho}{4-\rho^2} + \frac{32\rho\left[2-3\rho-2\,(2-\rho)\,(1-\rho)\,\frac{t}{\tau}\right]}{(2-\rho)^3\,(2+\rho)\left[2-(2-\rho)\,\frac{t}{\tau}\right]^2}\right]\mathrm{e}^{-(1+\rho/2)t/\tau} \\ &+ \frac{\mathrm{e}^{-\rho t/\tau}}{4\,(-4+\rho^2)}\left\{8\rho - 2\left[8-(4-\rho)\,\rho^2\right]\frac{t}{\tau} - (2-\rho)^2\left[4-\rho\,(2+\rho)\right]\left(\frac{t}{\tau}\right)^2\right\} \\ &+ \frac{4\rho\left[4\rho+(2-\rho)\,(2-3\rho)\,\frac{t}{\tau}\right]}{(2-\rho)^3\left[2-(2-\rho)\,\frac{t}{\tau}\right]^2}\mathrm{e}^{-2t/\tau} \\ &+ \frac{2\mathrm{e}^{-4/(2-\rho)}\rho}{(2-\rho)^4}\left[4-\rho\,(8+\rho)\right]\mathrm{Ei}\left(\frac{4}{2-\rho}-\frac{2t}{\tau}\right) \\ &+ \frac{8\mathrm{e}^{-(2+\rho)/(2-\rho)}\rho\left(-4+5\rho^2\right)}{(2-\rho)^4\,(2+\rho)}\mathrm{Ei}\left[\frac{2+\rho}{2-\rho}-\left(1+\frac{\rho}{2}\right)\frac{t}{\tau}\right],\end{aligned} \tag{25}$$

where $\mathrm{Ei}(z)$ is the exponential integral Ei [58]

$$\mathrm{Ei}(z) = \mathcal{P}\int_{-\infty}^{z}\frac{\mathrm{e}^t}{t}\mathrm{d}t. \tag{26}$$

In the long time limit the MSD converges to a constant, given by the first line of (25). If there are intervening particles, then the MSD must be lower than that given by (25). Therefore, the MSD of a totally persistent system converges to a density-dependent constant, bounded from above by (25). Figure 8 shows the value of the MSD at long times compared to the upper bound. We observe that the bound is indeed fulfilled. Remarkably, the upper bound provides a fairly good approximation to the simulated data at intermediate densities.

## 5. Full anti-persistence

In the complementary limit of full anti-persistence the system exhibits several unique properties. We consider a 1D lattice with totally anti-persistent particles, such that at each step the particles always switch direction and attempt to move in the opposite direction than before. To our knowledge, this pathological case has not been explored before. The two sites between which the particle hops change only if another particle enters one of the two sites, such that the first walker pushes itself on its new neighbour. Physically, this limit represents very deep and narrow traps, such that a particle can escape only if another particle enters its trap. In a closed system with density $\rho < 1/2$, we find that the system relaxes to a steady state in which each particle jiggles between two sites, and thus the MSD converges to a constant, see figure 9.

For $\rho > 1/2$ we find that the MSD scales as $\sqrt{t}$, as shown in figure 10(a). We extract the effective diffusion coefficient $D_{\mathrm{eff}}$ from the slope of the MSD versus time and show the results in figures 10(b) and (c). We note that unlike in the case with $\delta > -1/2$, here the MSD divided by $\sqrt{t}$ has a single maximum as a function of the density. At a density of exactly $\rho = 1/2$,

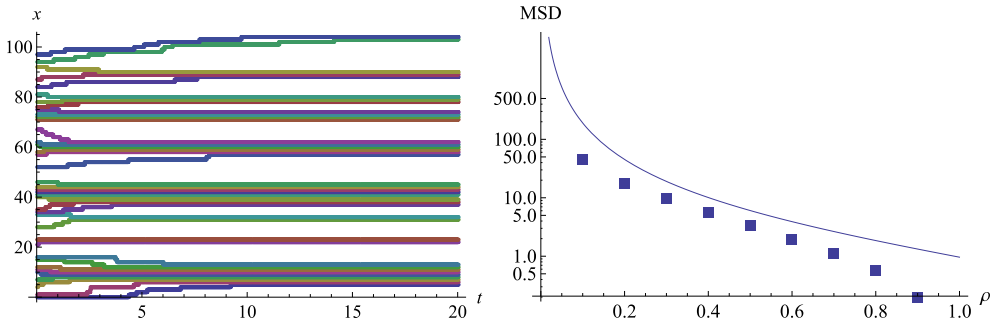


**Figure 8.** Totally persistent case. Left: sample trajectory of the system. Right: long time value of the MSD versus density. The symbols are simulations results, the continuous line is the analytical upper bound (25).

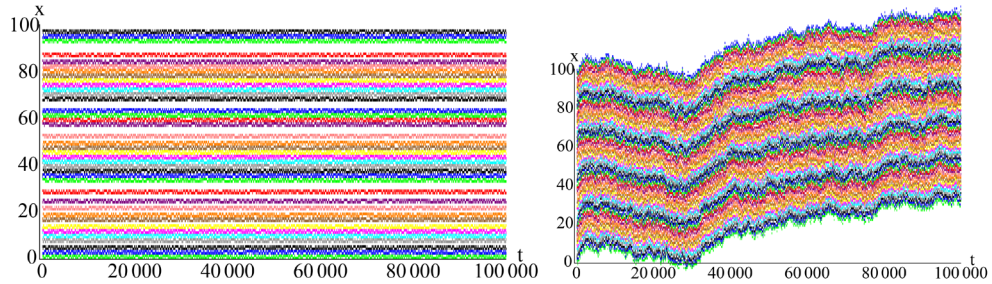


**Figure 9.** Time evolution of a fully anti-persistent system of length 100 with periodic boundary conditions, with either density $\rho = 0.4$ (left panel) or $\rho = 0.6$ (right panel). Each colour represents a different particle, and vacancies are represented in white. At low density, the particles are localised, while at the high density they move.

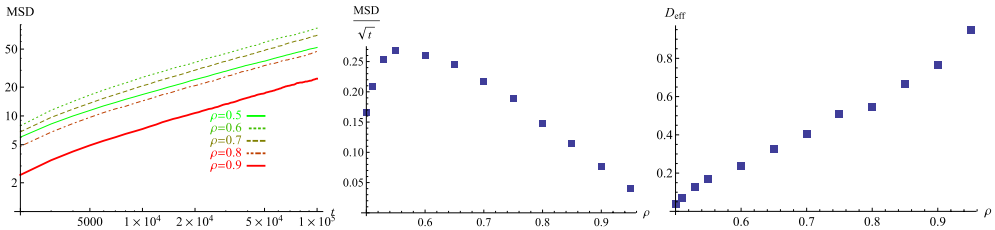


**Figure 10.** MSD and effective diffusion coefficient in the fully anti-persistent case for density $\rho \geqslant 0.5$.

the MSD appears to grow slightly slower than $\sqrt{t}$, however more precise measurements are required to find its exact time dependence.

## 6. Conclusions

We studied a lattice gas of persistent walkers in which each site is occupied by at most one particle and the direction each particle attempts to move to depends on its last step. The directionality is modulated by a 'persistence', the particle's tendency to continue moving in the

same direction as in the last step. Specifically, we analysed the mean squared displacement (MSD) as function of the particle density and the persistence.

First, we found that the scaling of the MSD with time is the same as in memory-less systems, i.e. the simple symmetric exclusion principle (SSEP) model, MSD$\propto \sqrt{t}$ in 1D and MSD$\propto t$ in 2D. We expect that this scaling remains true even for particles with longer memory, as long as the velocity autocorrelations decay sufficiently fast.

Second, we observed that the MSD increases with growing persistence of the walkers, in accordance with intuition. However, the dependence of the MSD on the density turns out to be non-trivial. As long as the anti-persistence, i.e. the tendency to go backwards, is not too high, the MSD decreases with the density $\rho$ simply due to the crowdedness. However, for highly anti-persistent walkers, the MSD *increases* with growing $\rho$ for low densities and reaches a *maximum* at some persistence-dependent density. This occurs because for highly anti-persistent walkers, the other walkers prevent a given walker from stepping backwards and thus effectively increase their MSD. There is also an intermediate regime in which for low densities the MSD decreases with the density, but at intermediate densities it reaches both a minimum and a maximum. To our knowledge, this type of behaviour has not been observed before.

Third, we considered the two extreme limits of full persistence and anti-persistence. For totally persistent particles, although a single walker performs a ballistic motion, when other particles come into play, the single walker is blocked by other particles going in the opposite direction, such that the MSD saturates and all movement halts. We derived an upper bound for the MSD in this case which quite nicely approximates the simulations results at intermediate particle densities. In the totally anti-persistent case, a single particle jumps between two sites, but when other particles exist and the density is higher than $\frac{1}{2}$, they enable it to move and the MSD grows as $\sqrt{t}$. We suspect that at exactly $\rho = \frac{1}{2}$ the MSD grows with time slower than $\sqrt{t}$, but more precise measurements are needed.

An interesting expansion of this work would be to analyse the MSD of walkers with slowly decaying velocity autocorrelations, in which the MSD of a single walker is not linear in time (anomalous diffusion [59]). In 1D a similar model was investigated in [51]. We expect that for positive autocorrelations (i.e. persistent walkers) the MSD in 1D scales as $\sqrt{t}$ for all densities, while for negative autocorrelations (i.e. anti-persistent walkers) it scales as $\sqrt{t}$ for $\rho > \frac{1}{2}$ and slower for $\rho < \frac{1}{2}$. From preliminary results on crowded Lévy walkers, we indeed find that in 1D the MSD scales as $\sqrt{t}$ and in 2D it scales as $t$. Furthermore, at high enough densities the system exhibits motiliy induced phase seperation (MIPS).

In the model we investigated here, the direction chosen at each step is completely uncorrelated to the success of failure of the moves and thus to the other particles. Another interesting expansion involves correlating the chosen direction with the density, such that the probability to move forward or backwards depends on whether the last move was successful or not. We conjecture that persistent walkers that tend to turn around when they are blocked would exhibit a transition from a behaviour similar to positive persistence at low densities to a behaviour similar to anti-persistence at high densities. Another expansion of this model would be to add quenched disorder to the system, i.e. to fix some of the particles in place so they become obstacles. It is possible that at sufficiently high densities, perhaps related to the percolation threshold, anti-persistent particles will have a higher MSD than persistent particles.

## Acknowledgments

We thank Yair Shokef, Michael Urbakh and Andrey Cherstvy for fruitful discussions. ET acknowledges financial support from the TAU-Potsdam fellowship. RM acknowledges the

Foundation for Polish Science (Fundacja na rzecz Nauki Polskiej) for funding within an Alexander von Humboldt Polish Honorary Research Scholarship, and DFG within Grants ME 1535/6-1 and 1535/7-1. We acknowledge the support of the Deutsche Forschungsgemeinschaft (German Research Foundation) and the Open Access Publication Fund of Potsdam University.

## Appendix. Calculation of the MSD in a mean field approximation

We here present a computationally efficient method of calculating the MSD in the mean field approximation. We derive the result for 1D systems, but expanding it to higher dimensions is straightforward. The derivation applies to more general models than we consider in this work.

Consider a single particle with a set of internal states moving in 1D. It is not constrained to move on a lattice. Given that it is currently at state $\eta$, it moves a distance $r$ and changes its state to $\eta'$ with rate $\mathcal{M}_{\eta,\eta'}(r)/\tau$. The evolution equation may be written in matrix form as

$$\tau\frac{\partial \mathbf{Q}(x,t)}{\partial t} = \int_{-\infty}^{\infty} \mathrm{d}r\mathcal{M}(r)\mathbf{Q}\left(x-r,t\right). \tag{A.1}$$

In Fourier space the evolution equation is given by

$$\tau\frac{\partial \tilde{\mathbf{Q}}(k,t)}{\partial t} = \mathcal{M}(k)\tilde{\mathbf{Q}}(k,t). \tag{A.2}$$

When $k=0$, the dynamical matrix has a single zero eigenvalue, with the corresponding right and left eigenvectors $\mathbf{V}_0$ and $\mathbf{U}_0^T$. Note that all entries of the left eigenvector are equal to 1, and the eigenvector $\mathbf{V}_0$ represents the steady state of the system. The other eigenvalues and eigenvectors are denoted by $\lambda_i$, $\mathbf{V}_i$ and $\mathbf{U}_i^T$ with $i>0$. The real part of all the other eigenvalues is negative. The solution to equation (A.2) is

$$\tilde{\mathbf{Q}}(k,t) = \mathrm{e}^{\mathcal{M}(k)t}\tilde{\mathbf{Q}}(k,0). \tag{A.3}$$

We assume that at time $t=0$ the system is in the steady state and the particle is at the origin (i.e. $\mathbf{Q}(n,0)=\delta_{n,0}\mathbf{V}_0$). Therefore, we note that at time $t=0$ the vector $\tilde{\mathbf{Q}}(k,0)$ is independent of $k$, since by definition

$$\tilde{\mathbf{Q}}(k,0) = \sum_{-\infty}^{\infty}\mathrm{e}^{\mathrm{i}nk}\mathbf{Q}(n,0) = \sum_{-\infty}^{\infty}\mathrm{e}^{\mathrm{i}nk}\delta_{n,0}\mathbf{V}_0 = \mathbf{V}_0. \tag{A.4}$$

The MSD is given by

$$\left\langle n^2\right\rangle = -\frac{\partial^2}{\partial k^2}\sum_{\sigma,\sigma_-,\sigma_+}\tilde{Q}_{\sigma,\sigma_-,\sigma_+}(k,t)\bigg|_{k=0} = -\frac{\partial^2}{\partial k^2}\mathbf{U}_0^T\mathrm{e}^{\mathcal{M}(k)t/\tau}\mathbf{V}_0\bigg|_{k=0}. \tag{A.5}$$

We now use [60]

$$\frac{\partial}{\partial k}\mathrm{e}^{\mathcal{M}(k)t/\tau} = \frac{t}{\tau}\int_0^1 \mathrm{e}^{\alpha\mathcal{M}(k)t/\tau}\frac{\partial\mathcal{M}(k)}{\partial k}\mathrm{e}^{(1-\alpha)\mathcal{M}(k)t/\tau}\mathrm{d}\alpha, \tag{A.6}$$

and find that

$$\langle n^2\rangle = -\frac{t}{\tau}\mathbf{U}_0^T\int_0^1\left\{\left[\int_0^1\alpha\frac{t}{\tau}\mathrm{e}^{\alpha\beta\mathcal{M}t/\tau}\frac{\partial\mathcal{M}}{\partial k}\mathrm{e}^{\alpha(1-\beta)\mathcal{M}t/\tau}\mathrm{d}\beta\right]\frac{\partial\mathcal{M}}{\partial k}\mathrm{e}^{(1-\alpha)\mathcal{M}t/\tau}\right.$$
$$+\mathrm{e}^{\alpha\mathcal{M}t/\tau}\frac{\partial\mathcal{M}}{\partial k}\left[\int_0^1(1-\alpha)\frac{t}{\tau}\mathrm{e}^{(1-\alpha)\beta\mathcal{M}t/\tau}\frac{\partial\mathcal{M}}{\partial k}\mathrm{e}^{(1-\alpha)(1-\beta)\mathcal{M}t/\tau}\mathrm{d}\beta\right]$$
$$\left.+\mathrm{e}^{\alpha\mathcal{M}t\tau}\frac{\partial^2\mathcal{M}}{\partial k^2}\mathrm{e}^{(1-\alpha)\mathcal{M}t/\tau}\right\}\mathrm{d}\alpha\mathbf{V}_0, \tag{A.7}$$

where the matrix $\mathcal{M}$ and its derivatives are evaluated at $k=0$. Since $\mathbf{V}_0$ and $\mathbf{U}_0^T$ are the zero eigenvalues of $\mathcal{M}$ at $k=0$ we find that

$$\langle n^2\rangle = -\frac{t}{\tau}\mathbf{U}_0^T\int_0^1\left\{\alpha\frac{t}{\tau}\frac{\partial\mathcal{M}}{\partial k}\left[\int_0^1\mathrm{e}^{\alpha(1-\beta)\mathcal{M}t/\tau}\mathrm{d}\beta\right]\frac{\partial\mathcal{M}}{\partial k}\right.$$
$$\left.+\frac{\partial\mathcal{M}}{\partial k}(1-\alpha)\frac{t}{\tau}\left[\int_0^1\mathrm{e}^{(1-\alpha)\beta\mathcal{M}t/\tau}\mathrm{d}\beta\right]\frac{\partial\mathcal{M}}{\partial k}+\frac{\partial^2\mathcal{M}}{\partial k^2}\right\}\mathrm{d}\alpha\mathbf{V}_0. \tag{A.8}$$

In the first term we change the integration variable from $\beta$ to $1-\beta$, in the second term we change the integration variable from $\alpha$ to $1-\alpha$, and in the third term we perform the integration over $\alpha$, such that

$$\langle n^2\rangle = -\frac{t}{\tau}\mathbf{U}_0^T\left\{2\frac{t}{\tau}\frac{\partial\mathcal{M}}{\partial k}\left[\int_0^1\int_0^1\alpha\mathrm{e}^{\alpha\beta\mathcal{M}t/\tau}\mathrm{d}\alpha\mathrm{d}\beta\right]\frac{\partial\mathcal{M}}{\partial k}+\frac{\partial^2\mathcal{M}}{\partial k^2}\right\}\mathbf{V}_0. \tag{A.9}$$

We now use the spectral decomposition of $\mathcal{M}$

$$\mathcal{M}=\sum_{i>0}\lambda_i\mathbf{V}_i\mathbf{U}_i^T, \tag{A.10}$$

such that

$$\mathrm{e}^{\alpha\beta\mathcal{M}t/\tau}=\mathbf{V}_0\mathbf{U}_0^T+\sum_{i>0}\mathrm{e}^{\alpha\beta\lambda_i t/\tau}\mathbf{V}_i\mathbf{U}_i^T. \tag{A.11}$$

We may now perform the integrals over $\alpha$ and $\beta$

$$\int_0^1\int_0^1\alpha\mathrm{e}^{\alpha\beta\mathcal{M}t/\tau}\mathrm{d}\alpha\mathrm{d}\beta=\frac{1}{2}\mathbf{V}_0\mathbf{U}_0^T+\sum_{i>0}\mathbf{V}_i\mathbf{U}_i^T\left[-\frac{1}{\lambda_i t/\tau}+\frac{\mathrm{e}^{\lambda_i t/\tau}-1}{(\lambda_i t/\tau)^2}\right], \tag{A.12}$$

which in the long time limit is

$$\int_0^1\int_0^1\alpha\mathrm{e}^{\alpha\beta\mathcal{M}t/\tau}\mathrm{d}\alpha\mathrm{d}\beta=\frac{1}{2}\mathbf{V}_0\mathbf{U}_0^T-\sum_{i>0}\mathbf{V}_i\mathbf{U}_i^T\frac{1}{\lambda_i t/\tau}. \tag{A.13}$$

We define a new matrix

$$\tilde{\mathcal{M}}=\mathcal{M}+\mathbf{V}_0\mathbf{U}_0^T, \tag{A.14}$$

such that

$$\int_0^1\int_0^1 \alpha e^{\alpha\beta\mathcal{M}t/\tau}d\alpha d\beta = \frac{1}{2}\mathbf{V}_0\mathbf{U}_0^T + \mathbf{V}_0\mathbf{U}_0^T\frac{1}{t/\tau} - \sum_{i>0}\mathbf{V}_i\mathbf{U}_i^T\frac{1}{\lambda_i t/\tau} - \mathbf{V}_0\mathbf{U}_0^T\frac{1}{t/\tau}$$
$$= \left(\frac{1}{2}+\frac{\tau}{t}\right)\mathbf{V}_0\mathbf{U}_0^T - \frac{\tau}{t}\tilde{\mathcal{M}}^{-1}, \tag{A.15}$$

and thus

$$\begin{aligned}\langle n^2\rangle = &-2\left(\frac{1}{2}+\frac{\tau}{t}\right)\left(\frac{t}{\tau}\right)^2\left(\mathbf{U}_0^T\frac{\partial\mathcal{M}}{\partial k}\mathbf{V}_0\right)^2 \\ &+2\frac{t}{\tau}\mathbf{U}_0^T\frac{\partial\mathcal{M}}{\partial k}\tilde{\mathcal{M}}^{-1}\frac{\partial\mathcal{M}}{\partial k}\mathbf{V}_0 - \frac{t}{\tau}\mathbf{U}_0^T\frac{\partial^2\mathcal{M}}{\partial k^2}\mathbf{V}_0.\end{aligned} \tag{A.16}$$

Due to symmetry the first term vanishes and thus

$$\langle n^2\rangle = 2\frac{t}{\tau}\mathbf{U}_0^T\frac{\partial\mathcal{M}}{\partial k}\tilde{\mathcal{M}}^{-1}\frac{\partial\mathcal{M}}{\partial k}\mathbf{V}_0 - \frac{t}{\tau}\mathbf{U}_0^T\frac{\partial^2\mathcal{M}}{\partial k^2}\mathbf{V}_0. \tag{A.17}$$

Note that in the case of isotropic one-step memory, all elements of the steady state distribution $\mathbf{V}_0$ are equal, and thus constructing the matrix $\mathbf{V}_0\mathbf{U}_0^T$ is trivial, and the only time consuming part of the calculation is the inversion of the matrix $\tilde{\mathcal{M}}$. It is straightforward to check that the MSD in a $d$ dimensional system is $d$ times the expression in (A.17).

## ORCID iDs

Ralf Metzler https://orcid.org/0000-0002-6013-7020

## References

[1] de Groot B L and Grubmüller H 2005 *Curr. Opin. Struct. Biol.* **15** 176
Höfling F and Franosch T 2014 *Rep. Prog. Phys.* **76** 046602
Bechinger C, Di Leonardo R, Löwen H, Reichhardt C, Volpe G and Volpe G 2016 *Rev. Mod. Phys.* **88** 045006
Metzler R, Jeon J H and Cherstvy A G 2016 *BBA-Rev. Biomembranes* **1858** 2451
Hakim V and Silberzan P 2017 *Rep. Prog. Phys.* **80** 076601
Nørregaard K, Metzler R, Ritter C M, Berg-Sørensen K and Oddershede L B 2017 *Chem. Rev.* **117** 4342
[2] Hasnain S and Bandyopadhyay P 2015 *J. Chem. Phys.* **143** 114104
[3] Detcheverry F 2015 *Europhys. Lett.* **111** 60002
Rupprecht J, Bénichou O and Voituriez R 2016 *Phys. Rev.* E **94** 012117
Detcheverry F 2017 *Phys. Rev.* E **96** 012415
[4] Sevilla F 2016 *Phys. Rev.* E **94** 062120
Ariel G, Be'er A and Reynolds A 2017 *Phys. Rev. Lett.* **118** 228102
Fedotov S and Korabel N 2017 *Phys. Rev.* E **95** 030107
[5] Wioland H, Lushi E and Goldstein R 2016 *New J. Phys.* **18** 075002
Stenhammer J, Nardini C, Nash R, Marenduzzo D and Mozorov A 2017 *Phys. Rev. Lett.* **119** 028005
[6] Berthier L and Kurchan J 2013 *Nat. Phys.* **9** 310
[7] Viscek T, Czirók A, Ben-Jacob E, Cohen I and Shochet O 1995 *Phys. Rev. Lett.* **75** 1226
Sepúlveda N, Petitjean L, Cochet O, Grasland-Mongrain E, Silberzan P and Hakim V 2013 *PLoS Comput. Biol.* **9** 1002944
Großmann R, Peruani F and Bär M 2016 *Phys. Rev.* E **94** 050602
Liebchen B and Levis D 2017 *Phys. Rev. Lett.* **119** 058002
[8] Zimmerman J, Camley B, Rappel W and Levine H 2016 *Proc. Natl Acad. Sci. USA* **113** 2660

[9] Farhadifar R, Röper J, Aigouy B, Eaton S and Jülicher F 2007 *Curr. Biol.* **17** 2095
Staple D, Farhadifar R, Röper J, Aigouy B, Eaton S and Jülicher F 2010 *Eur. Phys. J.* E **33** 117
Sándor C, Libál A, Reichhardt C and Reichhardt C 2017 *Phys. Rev.* E **95** 032606
[10] Reichhardt C and Reichhardt C 2014 *Soft Matter* **10** 7502
[11] Zacherson C, Wolff C, Whitchurch C and Toth M 2017 *Phys. Rev.* E **95** 012408
[12] Reichhardt C and Reichhardt C 2014 *Phys. Rev.* E **90** 012701
[13] Lam K, Schindler M and Dauchot O 2015 *New J. Phys.* **17** 113056
[14] Graf I and Frey E 2017 *Phys. Rev. Lett.* **188** 128101
[15] Illien P, Bénichou O, Oshanin G and Voituriez R 2015 *J Stat. Mech.* P11016
[16] Mark S, Shlomovitz R, Gov N, Poujade M, Grasland-Mongrain E and Silberzan P 2010 *Biophys. J.* **98** 361
McCalla S and Brecht J 2016 *Phys. Rev.* E **94** 060401
[17] Fisher H, Giomi L, Hoekstra H and Mahadevan L 2014 *Proc. R. Soc.* B **281** 20140296
[18] Berg H C and Turner L 1990 *Biophys. J.* **58** 919
[19] Schulz J, Kolomeisky A B and Frey E 2011 *Europhys. Lett.* **95** 30004
[20] Ghosh S K, Cherstvy A G and Metzler R 2015 *Phys. Chem. Chem. Phys.* **17** 1847
[21] Hermann C J J, Metzler R and Engbert R 2017 *Sci. Rep.* **7** 12958
[22] Taylor G 1921 *Proc. Math. Soc.* **2** 196
[23] Tchen C 1952 *J. Chem. Phys.* **20** 214
[24] Kareiva P and Shigesada N 1983 *Oecologia* **56** 234
[25] Boguña M, Porrá J and Masoliver J 1998 *Phys. Rev.* E **58** 6992
[26] Romanczuk P, Bär M, Ebeling W, Lindner B and Schminasky-Geier L 2012 *Eur. Phys. J.* **202** 1
[27] Ghosh P, Li Y, Marchgiani G and Marchesoni F 2015 *J. Chem. Phys.* **143** 211101
[28] Tahir-Kheli R A and Elliot R J 1983 *Phys. Rev.* B **27** 844
Tahir-Kheli R A 1983 *Phys. Rev.* B **27** 7229
[29] Spitzer F 1970 *Adv. Math.* **5** 246
[30] Melbinger A, Reichenbach T, Franosch T and Frey E 2011 *Phys. Rev.* E **83** 031923
[31] Gorissen M, Lazarescu A, Mallick K and Vanderzande C C 2012 *Phys. Rev. Lett.* **109** 170601
[32] Richards P M 1977 *Phys. Rev.* B **16** 1393
Brak R and Elliot R J 1989 *J. Phys.: Condens. Matter* **1** 10299
Derrida M, Evans M R, Hakim V and Pasquier V 1993 *J. Phys. A: Math. Gen.* **26** 1493
Honecker A and Peschel I 1997 *J Stat. Phys.* **88** 319
Lazarescu A and Mallick K 2011 *J. Phys. A: Math. Theor.* **44** 315001
[33] Waghe A, Rasaiah J C and Hummer G 2012 *J. Chem. Phys.* **137** 044709
[34] Yang S Y, Yang J A, Kim E S, Jeon G, Oh E J, Choi K Y, Hahn S K and Kim J K 2010 *ACS Nano* **4** 3817
[35] Song M S, Moon H C, Jeon J H and Park H Y 2018 *Nat. Commun.* **9** 344
Chen K J, Wang B and Granick S 2015 *Nat. Mater.* **14** 589
[36] Harris T 1965 *J. Appl. Probab.* **2** 323
[37] Spohn H 1983 *J. Phys. A: Math. Gen.* **16** 4275
[38] Illien P, Bénichou O, Mejìa-Monasterio C, Oshanin G and Voituriez R 2013 *Phys. Rev. Lett.* **111** 038102
Bénichou O, Illien P, Oshanin G, Sarracino A and Voituriez R 2014 *Phys. Rev. Lett.* **1113** 268002
Bénichou O, Illien P, Oshanin G, Sarracino A and Voituriez R 2018 *J. Phys.: Condens. Matter* **30** 443001
[39] Markham D C, Simpson M J, Maini P K, Gaffney E A and Baker R E 2013 *Phys. Rev.* E **88** 052713
[40] Arita C, Krapivsky P L and Mallick K 2014 *Phys. Rev.* E **90** 052108
[41] Szavitz-Nossan J, Romano M C and Ciandrini L 2018 *Phys. Rev.* E **97** 052139
[42] Ritort F and Sollich P 2003 *Adv. Phys.* **52** 219
[43] Whitelam S, Klymko K and Mandal D 2017 *J. Chem. Phys.* **148** 154902
[44] Soto R and Golestanian R 2014 *Phys. Rev.* E **89** 012706
[45] Treloar K K, Simpson M J and McCue S W 2011 *Phys. Rev.* E **84** 061920
[46] Kourbane-Houssene M, Erignoux C, Bodineau T and Tailleur J 2018 *Phys. Rev. Lett.* **120** 268003
[47] Manacorda A and Puglisi A 2017 *Phys. Rev. Lett.* **119** 208003
[48] Gavagnin E and Yates C A 2018 *Phys. Rev.* E **97** 32416
[49] Arita C and Ragoucy E 2018 *Phys. Rev.* E **98** 052118
[50] Galanti M, Fanelli D and Piazza F 2013 *Eur. Phys. J.* B **86** 456

[51] Sanders L, Lomholt M, Lizana L, Fogelmark K, Metzler R and Ambjörnsson T 2014 *New J. Phys.* **16** 113050
[52] Bertrand T, Illien P, Bénichou O and Voituriez R 2018 *New J. Phys.* **20** 113045
[53] Chatterjee R, Segall N, Merrigan C, Ramola K, Chakraborty B and Shokef Y 2019 *J. Chem. Phys.* **150** 144508
[54] Nakazato K and Kitahara K 1980 *Prog. Theor. Phys.* **64** 2261
Landim C, Olla S and Varadhan S R S 2001 *Commun. Math. Phys.* **224** 307
[55] Illien P, Bénichou O, Oshanin G, Sarracino A and Voituriez R 2018 *Phys. Rev. Lett.* **120** 200606
[56] Lizana L, Ambjörnsson T, Taloni A, Barkai E and Lomholt M A 2010 *Phys. Rev.* E **81** 051118
[57] Abramowitz M and Stegun I A 1972 *Handbook of Mathematical Functions* (Washington, DC: National Bureau of Standards) ch 6.5
[58] Abramowitz M and Stegun I A 1972 *Handbook of Mathematical Functions* (Washington, DC: National Bureau of Standards) ch 5.1
[59] Metzler R, Jeon J H, Cherstvy A G and Barkai E 2014 *Phys. Chem. Chem. Phys.* **16** 24128
[60] Wilcox R M 1967 *J. Math. Phys.* **8** 962